The minimum depth of fault failure in compressional environments

Eyal Stanislavsky and Grant Garven
Department of Earth and Planetary Sciences, Johns Hopkins University, USA

Received 30 September 2002; revised 4 October 2002; accepted 7 October 2002; published 19 December 2002.

[1] The absence of very shallow seismicity in thrust faults could be due to either a layered pore pressure/depth profile or to heterogeneous lithology of the crust. Poroelasticity equations were solved by the finite element discretization of a two-dimensional plane strain cross-section simulating a thrust environment. Although the modeled faults are actively compacting during thrusting, our numerical results show that the pore pressure accumulation in the basement is faster than in the fault zone and therefore the fluid flow is directed into the fault. The combination of heterogeneous rheology, with the existence of hydrostatic fluid, retards failure near the land surface. A layered pore pressure/depth profile, where the pore pressure is hydrostatic in the sediments and near lithostatic in the basement, magnifies this result and failure occurs faster. In fact, with this pore pressure/depth profile, failure is reached at the same depth regardless of the crustal structure we assume. *INDEX TERMS:* 7260 Seismology: Theory and modeling; 8020 Structural Geology: Mechanics; 8045 Structural Geology: Role of fluids; 8164 Tectonophysics: Evolution of the Earth: Stresses—crust and lithosphere. **Citation:** Stanislavsky, E., and G. Garven, The minimum depth of fault failure in compressional environments, *Geophys. Res. Lett.*, *29*(24), 2155, doi:10.1029/2002GL016363, 2002.

1. Introduction

[2] The distribution of earthquake depths defines the so-called "*seismogenic zone*" and is usually between 3–15 km depth [*Sibson*, 1982; *Scholz*, 1990]. The upper and lower limits of the seismogenic zone have been attributed to a geomechanical stability transition: the lower transition from unstable to stable slip is likely due to increasing temperature [*Brace and Byerlee*, 1970; *Tse and Rice*, 1986], and the upper transition from stable to unstable slip is likely due to stabilizing effects of low normal stress [*Dietrich*, 1978], lithological changes within the fault zone [*Marone and Scholz*, 1988] or temperature effects [*Blanpied et al.*, 1998].

[3] Another possible explanation for the absence of very shallow earthquakes is that the failure condition is never reached at these depths, even when the fault is not creeping. In this case the upper limit of the seismogenic zone is not a stability transition but instead marks the depth above which failure does not occur.

[4] Proximity of a fault to failure can be quantified using Coulomb failure stress (*CFS*) [*Harris and Simpson*, 1992; *Beeler et al.*, 2000]:

$$CFS = |\vec{\tau}| - \mu_s(\sigma_n - p) - C \qquad (1)$$

where $\vec{\tau}$ is the shear stress on the plane of the fault, μ_s is the coefficient of static friction, σ_n is the normal stress across the fault plane (positive for compressive stress), p is the pore pressure, and C is the cohesive strength of the fault. Zero or positive values of *CFS* imply that failure has been reached. A thrust fault with 30° dip angle will fail near the land surface because the normal stress on the fault decreases faster than the shear stress with decreasing depth [*Rudnicki and Wu*, 1995], assuming a homogeneous elastic half space with initial lithostatic stress, hydrostatic pore pressure gradient, and a constant horizontal tectonic load. Therefore, the absence of very shallow earthquakes cannot be explained by failure behavior in a simple homogeneous half space.

[5] In this paper we examine the upper limits for seismicity along pre-existing thrust faults. We find that the lack of very shallow seismicity can be explained by two reasons: 1) a specific pore pressure/depth profile and, 2) heterogeneous lithology of the country rock.

2. Hydromechanical Model

[6] To explore this problem, we formulate the force equilibrium equations using displacements and pore pressure as the primary variables [*Wang*, 2000]

$$G\nabla^2 u_i + \frac{G}{1-2\nu}\frac{\partial^2 u_k}{\partial x_i \partial x_k} = \alpha\frac{\partial p}{\partial x_i} - F_i \qquad (2)$$

where G is the shear modulus, u_i is the displacement in the i direction, ν is the drained Poisson's ratio, α is Biot's coefficient, p is the pore pressure, and F_i is the body force. The fluid mass conservation equation for saturated isothermal flow is [*Wang*, 2000]

$$\nabla \cdot \left(-\frac{k_{ij}}{\mu}\nabla\left(p + \rho_f g z\right)\right) = \alpha\frac{\partial \varepsilon_{kk}}{\partial t} + S_\varepsilon\frac{\partial p}{\partial t} \qquad (3)$$

where k_{ij} is the permeability of the medium, μ is the fluid viscosity, ρ_f is the fluid density, ε_{kk} is the volumetric strain, and S_ε is the specific storage at constant strain. The poroelasticity equations were solved by the finite element method for a two-dimensional, plane strain, cross-section, closely following the formulation of *Lewis and Schrefler* [1987]. *CFS* was calculated along the existing faults within the cross-section, assuming representative values of μ = 0.75 and C = 10 MPa [*Byerlee*, 1967; *Handin*, 1969; *Byerlee*, 1978; *Jaeger and Cook*, 1979, *Lockner*, 1995; *Zoback and Townend*, 2001].

[7] A generic continental domain was discretized with a mesh covering a region 75 km long and 14 km deep that includes two very large thrust planes which crosscut sedimentary beds and crystalline basement (Figure 1). Assumed

0094-8276/02/2002GL016363$05.00

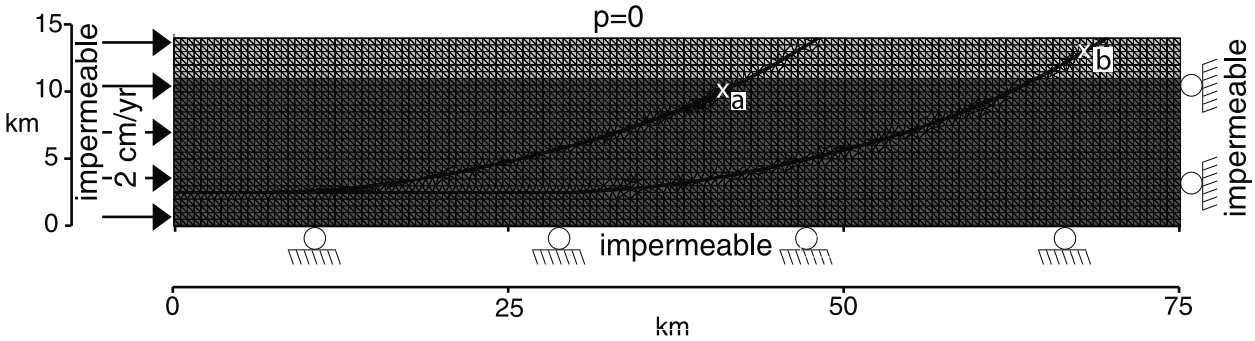

Figure 1. Numerical mesh and boundary conditions. The lithological units include sediment layer, basement and two thrust faults. The hydrologic boundary conditions include p = 0 top boundary (water table) and impermeable lower and horizontal boundaries. The mechanical boundary conditions: left boundary subjected to an imposed velocity of 2 cm/yr rightwards and unconstrained vertical displacement, bottom boundary free to move horizontally and fixed vertically, right boundary free to move vertically and fixed horizontally, and top boundary free to move in all directions.

hydraulic and poroelastic properties, as listed in Table 1, are based on compiled measurements for sandstone and granite [*Detournay and Cheng*, 1993; *Ingebritsen and Manning*, 1999; *Wang*, 2000]. The elastic properties of the thrust faults are assumed to be the same as for the sediments. Fault parameters are difficult to determine and direct measurements are rare [*Antonellini and Aydin*, 1994; *Caine and Forster*, 1999]. Although the porosity of faults is not well constrained, it is well accepted that the creation of fault gouge during fault slip, along with healing and sealing of the fault, result in a general reduction of the fault permeability and porosity (*Blanpied et al.*, 1992). In Figure 1, the faults are nearly impermeable barriers for fluid flow except immediately after rupture, after which they briefly become highly permeable channelways for fluid discharge [*Sibson*, 1992]. We consider only the inter-seismic period, assuming initial lithostatic stress until the first failure. Initially, the permeability of the faults is the same as the surrounding host rock (Table 1). The mechanical properties of the faults and the sedimentary layer are identical, whereas the basement is more rigid. The top boundary is open to the atmosphere and the bottom and lateral sides are assumed to be impermeable.

[8] Mechanically, the left boundary is subjected to an imposed velocity of 2 cm/yr to the right with unconstrained vertical displacement; the bottom boundary is free to move horizontally but fixed vertically; the right boundary is free to move vertically, but fixed horizontally. The top boundary is free to move in all directions. Many different initial pore pressure profiles, boundary conditions, and material properties were tested, but only a few of the more interesting results are presented here.

3. Numerical Results

[9] Because the top layer and the faults have exactly the same initial elastic properties, the pore pressure and the effective stress have about the same values within and outside the fault after 6,000 years of tectonic compression, representing 120 meters of lateral shortening (Figure 2). The basement, however, which is more rigid, develops higher pore pressures and stresses (Figures 2a, 2b, 2c). This result is at variation with models proposed by *Byerlee* [1990] and *Rice* [1992] who showed that a "*weak*" San-Andreas fault could be explained by high fluid pressure in the fault. In our simulation, the displacements are about the same order of magnitude everywhere (using velocity boundary conditions), and therefore the magnitude of elastic constants control the magnitude of the pore pressure (equation 2). At high values (rigid) the pore pressure and the stress are high, and at low values (soft) the pore pressure and the stress are low. Even though the faults are actively compacting, the pore pressure accumulation in the surrounding basement rock is faster than in the fault zone and therefore the fluid flow is focused into the fault. The horizontal effective stress is higher than the vertical effective stress (note the different scales) because of the horizontal compression. The vertical stress is approximately the overburden load because the top boundary is free so there is no stress added to the vertical direction. Vertical effective

Table 1. Simulation parameters[a]

Model Properties	Sediments	Basement	Faults
Shear Modulus [GPa]	6.0	15.0	6.0
Poisson's Ratio [−]	0.20	0.25	0.20
Undrained Poisson'sRatio [−]	0.33	0.34	0.33
Skempton's Coefficient [−]	0.62	0.85	0.62
Initial Permeability [m^2]	$k_{xx} = 10^{-16}$ $k_{zz} = 10^{-18}$ $k_{xz} = 0$	$\log k_{xx} = -14-3.2\log z$ $k_{zz} = k_{xx}/50$ $k_{xz} = 0$	equal to the host rock permeability
Initial Porosity [−]	0.15	0.05	0.02

[a]Mechanical properties are based on tabulation in *Detournay and Cheng* [1993], and *Wang* [2000]. Basement permeability is based on compilations in *Ingebritsen and Manning* [1999].

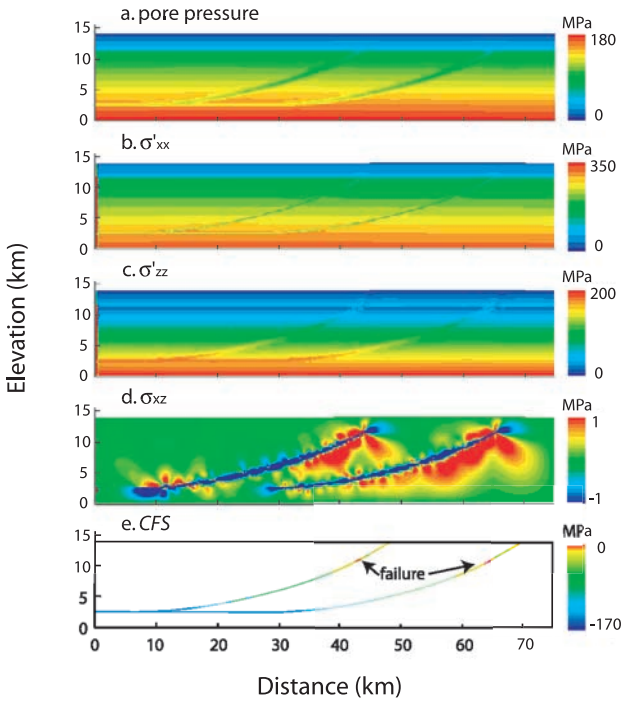

Figure 2. A snapshot of the finite element modeling after 6,000 years of tectonic compression assuming initial hydrostatic pore pressure and lithostatic stress (note the different scales): (a) pore pressure distribution, (b) effective horizontal stress σ'_{xx}, (c) effective vertical stress σ'_{zz} (d) cross term σ_{xz}, and (e) Coulomb failure stress (*CFS*). Fluids within the faults and in the basement are overpressured and the pore pressure and the stresses in the basement are higher than within the fault. Failure occurs at depth of 4 km.

stress is higher in the faults than in the basement because the pressure is lower (Figure 2c). The pore pressure and the effective vertical stress have about the same values so that the total vertical stress is the sum of these two quantities, and thus hydrofracturing does not occur. At initial isostatic stress (i.e. $\sigma_1 = \sigma_2 = \sigma_3$), the principal axes of the stress tensor are horizontal and vertical ($\sigma_{xz} = 0$). With loading, because of contrasts in mechanical properties of the different lithological units and because of the pore pressure accumulation, shear is introduced, and the orientation of principal stresses is rotated (Figure 2d), as discussed by *Rice* [1992] and *Byerlee* [1992]. The complex pattern arises because the slope of the fault is constant in an element but is changing between elements. The larger the *CFS* is, the closer the fault is to failure (Figure 2e). In this case the fault failed at depth of 4 km. The transient *CFS* evolution at two points within the fault zone (a and b at Figure 1) is shown in Figure 3. Although the initial *CFS* at the shallower point is closer to failure, the fault eventually fails after 6,000 years at the deeper point, because at this point the host rock is more rigid and the *CFS* is changing faster. In this model the slope of the faults is decreasing from an optimally oriented 30° at the land surface to 0° at depth of 11 km. The failure occurs at a depth of 4 km in spite of the changing slope.

[10] In the scenario of a dry cross-section with the mechanical properties listed in Table 1, failure of the fault occurs at the top land surface. For a geologically homogeneous cross-section with faults and hydrostatic pore pressure, failure also occurs at the land surface. The combination of heterogeneous mechanical properties as shown in Figure 1, with the influence of fluid pressure, retards failure near the surface, but different pore pressure/depth profiles also alter the failure location. For example, if the pore pressure is hydrostatic in shallow layers and near lithostatic (λ_v = fluid pressure/solid vertical stress = 0.9) in deeper layers, then the fault fails at the transition zone between the two regimes even for a mechanically homogeneous cross-section. Under this scenario, the fault will fail after 4,000 years at the same location, as when the initial pore pressure was hydrostatic everywhere (compare with 6,000 years for initial hydrostatic pore pressure).

4. Discussion

[11] Elevated pore pressures reduce the effective normal stress throughout a rock mass and thereby reduce the shear strength of faults [*Hubbert and Rubey*, 1959]. Hydrostatic fluid pressures exist at shallow depths in many basins, whereas overpressured fluids exist below [*Bredehoeft and Hanshaw*, 1968; *Berry*, 1973; *Bradley*, 1975; *Neuzil*, 1995; *Tóth and Almási*, 2001]. *Streit* [1997] calculated strength/depth profiles based on a fault valve model [*Sibson*, 1992] and showed that the location of the strength minimum depends on the pore pressure/depth profile. The strength minimum is reached where a near-lithostatic fluid pressure is attained. However, in strength/depth calculations the actual shear stress of the fault is not known and the failure location is assumed to be at the strength minimum, but it is not calculated. The actual failure condition (*CFS*) could not be calculated without considering the shear stress along the fault.

[12] Our numerical results show that by using the same initial pore pressure/depth profile as suggested by *Streit* [1997], failure is indeed reached where a near-lithostatic fluid pressure is attained. However, when using a different initial pore pressure/depth profile where the pore pressure is

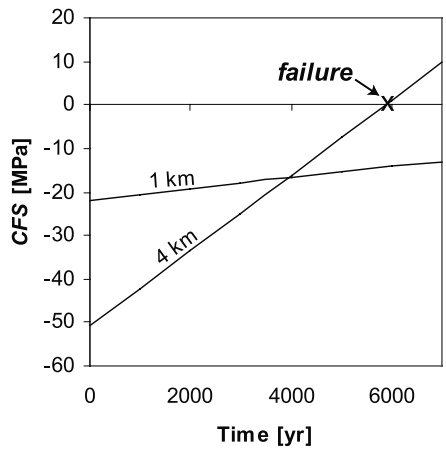

Figure 3. The transient *CFS* evolution at two reference points within the fault zone (a and b in Figure 1). Although the initial *CFS* at the shallower point is closer to failure, the fault eventually fails at the deeper point because at this point the host rock is more rigid and the *CFS* is changing faster.

hydrostatic everywhere, there is no strength minimum and yet failure occurs at the same depth due to different mechanical properties of the layered crust. If a sedimentary basin is subjected to tectonic loading and a fault zone within the basin is much softer mechanically than the host rock (basement), then most of the deformation takes place at the fault zone. Consequently, high stresses develop within the fault zone, though less than in the host rock (Figures 2b and 2c). If the fault zone rigidity is the same order of magnitude as the host rock (sediments), then the deformation will be transmitted more equally between the fault and the host rock and thereby decrease the stress within the fault (Figures 2b and 2c). Failure on the fault will occur, therefore, first in the basement where the stress is higher (Figure 2e).

5. Conclusions

1. Although fault creep is known to exist in some faults and is commonly cited as the reason for the absence of very shallow earthquakes, our poroelastic analysis suggests that thrust faults fail at depths greater than 3 km because of a pore pressure/depth profile that is not hydrostatic or because of mechanically heterogeneous crust. Each by itself could be solely responsible for the paucity of very shallow earthquakes.

2. For a representative geological cross-section where basin sediments overlay crystalline basement, the pressure of pore fluids with a uniform hydrostatic pore pressure gradient is sufficient by itself to change the failure location of a thrust fault from near the land surface to the basement. The thrust fault in the relatively soft sediment with low pore pressure has correspondingly low values of *CFS*, yet it fails in the more rigid basement with higher pore pressure. A different pore pressure/depth profile, where the pore pressure is hydrostatic in the sediments and near lithostatic in the basement, magnifies this result and failure occurs faster. In fact, with this pore pressure/depth profile, failure is reached at the same depth regardless of the crustal structure we assume.

3. The coupled numerical model predicts pore pressures that are higher in the host sedimentary and crystalline rock than in the thrust faults, even though both are overpressured.

[13] **Acknowledgments.** The research reported in this paper was supported by funding from the Department of Energy (DE-FGO2-96ER14619). The authors appreciated the long and helpful discussions with Peter Olson and useful comments from John Rudnicki and Ze'ev Reches. We are grateful to Stephen F. Cox, Chris Neuzil, and two anonymous experts whose reviews helped us improve the manuscript.

References

Antonellini, M., and A. Aydin, Effects of faulting on fluid flow in porous sandstones: petrophysical properties, *AAPG Bull.*, *78*, 355–377, 1994.

Beeler, N. M., R. W. Simpson, S. H. Hickman, and D. A. Lockner, Pore fluid pressure, apparent friction, and Coulomb failure, *J. Geophys. Res.*, *105*, 25,533–25,542, 2000.

Berry, F. A. F., High fluid potentials in the California Cost Ranges and their tectonic significance, *AAPG Bull.*, *57*, 1219–1249, 1973.

Blanpied, M. L., D. A. Lockner, and J. D. Byerlee, An earthquake mechanism based on rapid sealing of faults, *Nature*, *358*, 574–576, 1992.

Blanpied, M. L., C. J. Marone, D. A. Lockner, J. D. Byerlee, and D. P. King, Quantitative measure of the variation in fault rheology due to fluid-rock interactions, *J. Geophys. Res.*, *103*, 9691–9712, 1998.

Bredehoeft, J. D., and B. B. Hanshaw, On the maintenance of anomalous fluid pressure: I, Thick sedimentary sequences, *Geol. Soc. Am. Bull.*, *79*, 1097–1106, 1968.

Brace, W. F., and J. D. Byerlee, California earthquakes: Why not shallow focus?, *Science*, *168*, 1573–1575, 1970.

Bradley, J. S., Abnormal formation pressure, *AAPG Bull*, *59*, 957–973, 1975.

Byerlee, J. D., Friction of rocks, *Pure Appl. Geophys.*, *116*, 615–626, 1978.

Byerlee, J. D., Frictional characteristics of granite under high confining pressure, *J. Geophys. Res.*, *72*, 3639–3648, 1967.

Byerlee, J. D., Friction, overpressure and fault normal compression, *Geophys. Res. Lett.*, *17*, 2109–2122, 1990.

Byerlee, J. D., The change in orientation of subsidiary shears near faults containing pore fluid under high pressure, *Tectonophysics*, *211*, 295–303, 1992.

Caine, J. S. and C. B. Forster, Fault zone architecture and fluid flow: Insights from field data and numerical modeling, in *Faults and Subsurface Fluid Flow in the Shallow Crust*, edited by W. C. Haneberg, P. S Mozley, J. C. Moore, and L. B. Goodwin, Geophys. Monog. 113, 101–127, 1999.

Detournay, E. and A. H. D. Cheng, Fundamentals of poroelasiticity, in *Comprehensive Rock Engineering*; *Principles*, *Practice and Projects*, *II*, edited by J. A. Hudson, Pergamon Press, Oxford, UK, 113–171, 1993.

Dietrich, J., Time-dependent friction and the mechanics of stick-slip, *Pure Appl. Geophys.*, *116*, 790–806, 1978.

Handin, J., On the Coulomb-Mohr failure criterion, *J. Geophys. Res.*, *74*, 5343–5348, 1969.

Harris, R. A., and R. W. Simpson, Changes in static stress on southern California faults after the 1992 Landers earthquake, *Nature*, *360*, 313–318, 1992.

Hubbert, M. K., and W. W. Rubey, Role of fluid pressure in mechanics of overthrust faulting, *Geol. Soc. Am. Bull.*, *70*, 115–206, 1959.

Ingebritsen, S. E., and C. E. Manning, Geological implications of a permeability-depth curve for the continental crust, *Geology*, *27*, 1107–1110, 1999.

Jaeger, J. C., and N. G. W. Cook, *Fundamentals of Rock Mechanics*, Chapman and Hall, New York, 1979.

Lewis, R. W., and B. A. Schrefler, *The Finite Element Method in the Deformation and Consolidation of Porous Media*, 492 pp., John Wiley & Sons, New York, 1987.

Lockner, D. A., Rock failure, in *Rock Physics and Phase Relations, A Handbook of Physical Constants*, edited by T. J. Ahrens, AGU., 127–147, 1995.

Marone, C., and C. H. Scholz, The depth of seismic faulting and the upper transition from stable to unstable slip regimes, *Geophys. Res. Lett.*, *15*, 621–624, 1988.

Neuzil, C. E., Abnormal pressures as hydrodynamic phenomena, *Am. J. Sci.*, *295*, 742–786, 1995.

Rice, J. R., Fault stress states, pore pressure distribution, and the weakness of the San Andreas Fault, in *Fault mechanics and transport properties of rocks*, edited by B. Evans and T.-F. Wong, Academic, San Diego, Calif., pp. 475–503, 1992.

Rudnicki, J. W., and M. Wu, Mechanics of dip-slip faulting in an elastic half-space, *J. Geophys. Res.*, *100*, 22,173–22,186, 1995.

Scholz, C. H., *The Mechanics of Earthquakes and Faulting*, Cambridge Univ. press, New York, 1990.

Sibson, R. H., Fault zone models, heat flow, and the depth distribution of earthquakes in the continental crust of the united states, *Bull. Seismol. Soc. Am.*, *72*, 151–163, 1982.

Sibson, R. H., Implication of fault-valve behavior for rupture nucleation and recurrence, *Tectonophysics.*, *211*, 283–293, 1992.

Streit, J. E., Low frictional strength of upper crustal fault: A model, *J. Geophys. Res.*, *102*, 24,619–24,626, 1997.

Tóth, J., and I. Almási, Interpretation of observed fluid potential patterns in a deep sedimentary basin under tectonic compression: Hungarian Great Plain, Pannonian Basin, *Geofluids*, *1*, 11–36, 2001.

Tse, S. T., and J. R. Rice, Crustal earthquake instability in relation to the depth variation of frictional slip properties, *J. Geophys. Res.*, *91*, 9452–9472, 1986.

Wang, H. F., *Theory of Linear Poroelasticity with Applications to Geomechanics and Hydrogeology*, Princeton University Press, 2000.

Zoback, M. D., and J. Townend, Implications of hydrostatic pore pressure and high crustal strength for the deformation of intraplate lithosphere, *Tectonophysics*, *336*, 19–30, 2001.

E. Stanislavsky and G. Garven, Department of Earth and Planetary Sciences, Johns Hopkins University, USA.